

# Any-time Trajectory Planning for Safe Emergency Landing

Petr Váňa\*

Jakub Sláma\*

Jan Faigl

Pavel Pačes

**Abstract**—Loss of thrust is a critical situation for human pilots of fixed-wing aircraft which force them to select a landing site in the nearby range and perform an emergency landing. The time for the landing site selection is limited by the actual altitude of the aircraft, and it may be fatal if the correct decision is not chosen fast enough. Therefore, we propose a novel RRT\*-based planning algorithm for finding the safest emergency landing trajectory towards a given set of possible landing sites. Multiple landing sites are evaluated simultaneously during the flight even before any mechanical issue occurs, and the roadmap of possible landing trajectories is updated permanently. Thus, the proposed algorithm has the any-time property and provides the best emergency landing trajectory almost instantly.

## I. INTRODUCTION

A powerplant failure was the most common mechanical cause of non-commercial fixed-wing aircraft accidents in 2014 when 63 of them were documented [1] and, unfortunately, 12 of them were fatal. In the same year, about 80% of all fatal accidents involved in-flight losses of thrust caused by various problems, such as a mechanical problem, bird strike, or fuel exhaustion. Probably the most publicly known event happened in 2009 when US Airways Flight 1549 encountered a flock of birds and lost both engines [2]. The pilots had only tens of seconds to select a landing site. After they inspected all airports nearby, the time for their decision was over, and they were forced to land on the Hudson River. Fortunately, all the lives on-board were saved. Later simulations suggested that there was a chance to avoid water ditching and land safely at the LaGuardia Airport up to about 30 seconds after the unexpected bird strike [3]. However, such a decision is hard to be “computed” by human pilots under stress and such a time pressure when the source of the technical problem itself has to be identified and responded adequately.

Developing a system that will support the pilots’ decisions based on all the currently available computational machinery is our motivation to study the herein presented trajectory planning for an emergency landing. Thus, we aim to provide pilots fast and reliable information about possible landing sites, and we propose a novel method for emergency trajectory planning in a case of the total loss of thrust (LoT) scenarios. In the LoT situation, the aircraft starts to glide, and the pilot is forced to choose the most suitable landing site. The problem is visualized in Fig. 1.

The presented work has been supported by the Czech Science Foundation (GAČR) under research project No. 16-24206S. The authors acknowledge the support of the OP VVV funded project CZ.02.1.01/0.0/0.0/16\_019/0000765 “Research Center for Informatics”.

The authors are with the Faculty of Electrical Engineering, Czech Technical University in Prague, Technická 2, 166 27 Prague, Czech Republic {vanapet1|slamajak|faigl|j|pacesp}@fel.cvut.cz

\*The first two authors contributed equally to this work.

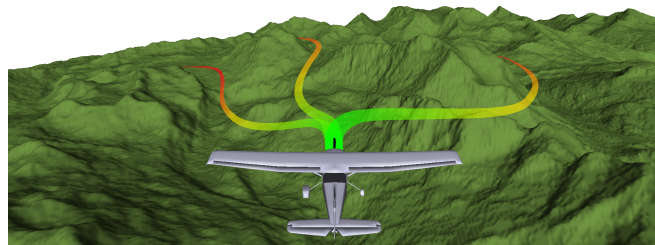


Fig. 1. Visualization of the problem of selecting the best landing site for the total loss of thrust situation. In such a case, pilots have to choose the best landing site and a trajectory towards it as quickly as possible.

The most direct approach to find an emergency glide trajectory is to utilize the shortest path generated in 2D concerning the minimum turning radius of the aircraft. For such a case, Dubins maneuvers [4] with its closed-form solution can be utilized. The maneuvers can be further extended into the 3D considering the highest possible glide ratio of the specific aircraft, and additional spiral segments inserted if it is necessary to lose spare altitude. This concept is known as the Dubins Airplane model [5] which is utilized in [3] with a discrete set of turning radii to calculate glide trajectories for the Hudson River accident.

On the other hand, [3] considers only direct trajectories without any collision with the ground obstacles (buildings, power lines, trees, etc.) or the terrain. To encounter the obstacles, a hybrid A\* algorithm is proposed in [6] and several other approaches, such as RRT\* or genetic algorithms were studied in [7]. Similar approaches can be applied even to the emergency trajectory planning of rotary-wing aircraft [8]. If no airport is close enough and an alternative landing site needs to be selected [9], [10], [11]; however, such an extension is out of the scope of this paper.

Existing approaches [7], [8] are designed to start the trajectory planning at the moment a mechanical problem occurs and consider a fixed planning time. In contrast, we are proposing an any-time planning approach based on the Informed RRT\* [12] in which possible trajectories to multiple landing sites are examined simultaneously, and the algorithm is launched during the aircraft take-off and run during the whole flight. It enables to retrieve an emergency landing trajectory instantly when necessary. The proposed any-time concept also provides the pilot with extra information during the flight, such as the current number of available landing sites or the minimum safety altitude to reach at least one landing site. Moreover, a detailed energy model of gliding is utilized, and the radius of each maneuver is optimized to find trajectories with the lowest altitude loss. The main contributions of the paper are considered as follows.

- Continuous optimization of the turning radius.
- Novel any-time informed trajectory planning algorithm for multiple landing sites based on the Informed RRT\*.
- Comparison of the proposed any-time algorithm to its single-query variant inspired by [3].

The rest of the paper is organized as follows. The problem is formally introduced in the next section. The utilized model of the gliding aircraft together with the turning radius optimization is described in Section III. The proposed any-time emergency landing planning algorithm based on the Informed RRT\* is described in Section IV and results of its evaluation in realistic scenarios are reported in Section V. The conclusion and final remarks are in Section VI.

## II. PROBLEM STATEMENT

The studied problem stands to find a safe emergency landing trajectory in a case the aircraft encounters an unexpected loss of thrust (LoT), and the pilot is forced to select the most suitable landing site. The trajectory is selected such that the minimum height above the terrain is maximized to provide the pilot enough time and space for a safe landing. Such a planned trajectory ends above the selected landing site because the aircraft is assumed to be able to lose the altitude significantly faster if necessary and losing altitude is much easier and safer than flying closely above the terrain. Moreover, this concept gives the best chance to pilot to solve other unexpected issues, such as bad weather conditions.

The state of the aircraft is given by its configuration  $q = (x, y, z, \psi, \theta, \varphi, V)$  where  $(x, y, z)$  is the aircraft position in the 3D, the angle  $\psi$  is the heading angle,  $\theta$  is the pitch angle,  $\varphi$  is the roll angle, and  $V$  is the forward speed. Thus,  $q$  is in the configuration space  $\mathcal{C} = \mathbb{R}^4 \times \mathbb{S}^3$  which has seven dimensions in the total. The motion of the aircraft is constrained by the minimum turning radius, and the pitch angle is influenced by the thrust of the motor and the selected trajectory curvature to preserve the constant speed  $V$ .

A set of  $n$  landing sites  $\Xi = \{\xi_1, \dots, \xi_n\}$  is given and each site is defined by the expected final configuration  $q^{\xi_i}$  of an aircraft at the site. Let  $\Gamma$  be an emergency landing trajectory  $\Gamma : [0, 1] \rightarrow \mathcal{C}$  that starts at the current aircraft configuration  $q_{\text{act}}$ , i.e.,  $\Gamma(0) = q_{\text{act}}$ . The end of  $\Gamma$  is selected from a set  $\hat{\xi}_*$  containing all configurations directly above the selected landing site  $\xi_* \in \Xi$  which correspond to the configuration  $q^{\xi_*}$  of the selected site, i.e.,  $\Gamma(1) \in \hat{\xi}_*$ .

Let  $\mathcal{T}_{\text{alt}} : \mathbb{R}^2 \rightarrow \mathbb{R}$  be the minimum altitude for the aircraft without any collision with the terrain or the obstacles at the specific position  $(x, y)$ . The problem of selecting the best landing site  $\xi_*$  with the corresponding landing trajectory  $\Gamma$  can be formulated as the problem to find  $\Gamma$  that maximizes the minimum height of the aircraft above the terrain or obstacles

$$h_{\min} = \min_{t \in [0, 1]} \Gamma_z(t) - \mathcal{T}_{\text{alt}}(\Gamma_{2D}(t)), \quad (1)$$

where  $\Gamma_z(t)$  stands for the altitude  $z$  of the trajectory  $\Gamma$  at  $t$  and  $\Gamma_{2D}(t)$  is the 2D position  $(x, y)$  of the trajectory at  $t$ . Then, the safest landing trajectory is the trajectory such that the value of  $h_{\min}$  is maximized, and thus we are searching

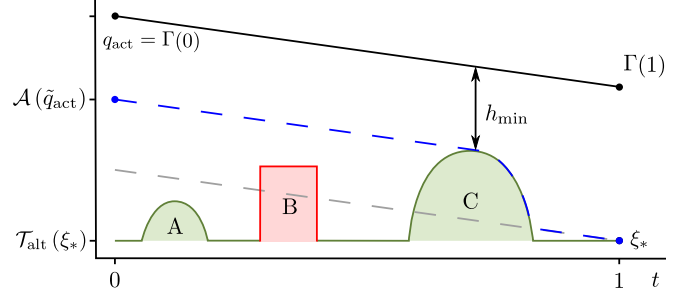


Fig. 2. An example of the optimization criteria  $h_{\min}$  for the trajectory  $\Gamma$  which maximizes the safety of the glide landing trajectory (black line) by maximizing the minimum height of the aircraft above the terrain. The value of  $h_{\min}$  is influenced by the hill C where the blue dashed line represents the minimum altitude  $\mathcal{A}$  for a safe landing.

for the landing site  $\xi_*$  and the landing trajectory  $\Gamma$  that maximizes (1). An example of  $h_{\min}$  with possible landing trajectories is shown in Fig. 2.

*Problem 2.1 (Planning Safe Emergency Landing):*

$$\begin{aligned} \max_{\Gamma, \xi_* \in \Xi} \quad & h_{\min} & (2) \\ \text{s.t.} \quad & \Gamma(0) = q_0, \Gamma(1) \in \hat{\xi}_*. & (3) \end{aligned}$$

The crucial part of the emergency trajectory planning is the model of the altitude loss for the specified 2D trajectory of the aircraft. In this work, the difference in the altitudes between two configurations is expressed by the following equation for  $t_1, t_2 \in [0, 1], t_1 < t_2$

$$\Gamma_z(t_1) - \Gamma_z(t_2) = \mathcal{H}(\Gamma(t_1), \Gamma(t_2)), \quad (4)$$

where  $\mathcal{H}$  is a function of the altitude loss. The particular altitude loss function is detailed in the next section, where the radius is optimized to reduce the total altitude loss.

## III. MODEL OF THE GLIDING AIRCRAFT AND ALTITUDE LOSS FUNCTION

LoT forces the pilot to glide, and the goal is to minimize the total altitude loss by choosing the trajectory and by adjusting the utilized turning radii. The dynamic of the aircraft is influenced mainly by the thrust  $\mathbf{T}$ , drag  $\mathbf{D}$ , weight  $\mathbf{W}$ , and lift  $\mathbf{L}$ , see Fig. 3. For a steady flight, all these forces cancel out, and the resultant force is zero. Assuming the flight to be in the standard envelope [13], the magnitudes of these forces are influenced by the lift coefficient  $C_L$  and drag coefficient  $C_D$  given by

$$L = \|\mathbf{L}\| = \frac{1}{2} \rho C_L S V^2, \quad D = \|\mathbf{D}\| = \frac{1}{2} \rho C_D S V^2, \quad (5)$$

where  $S$  is the wing reference area. The drag coefficient  $C_D$  depends on the zero-lift drag coefficient  $C_{D0}$ , lift-induced drag coefficient  $k$ , and lift coefficient  $C_L$  given by

$$C_D = C_{D0} + k C_L^2, \quad k = \frac{S}{\pi b^2 \epsilon}, \quad (6)$$

where  $S$  is the wing reference area,  $b$  is the wing span, and  $\epsilon$  is the span efficiency factor.

The state of an aircraft is given by its position  $(x, y, z)$ , heading angle  $\psi$ , pitch angle  $\theta$ , roll angle  $\varphi$ , and magnitude  $V$  of the airspeed. Two assumptions are made to

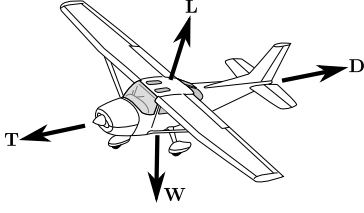


Fig. 3. Forces acting on an aircraft. Both drag  $\mathbf{D}$  and thrust  $\mathbf{T}$  act in parallel with direction of flight, weight  $\mathbf{W}$  acts vertically and lift  $\mathbf{L}$  is perpendicular to the wing's plane.

simplify the aircraft model. First, the pitch angle  $\theta$  is equal to the angle of descent, i.e., the angle of attack is zero. Secondly, all maneuvers are considered to be smooth and coordinated, and thus the sideslip is zero. Thus, the bank angle equals the roll angle  $\varphi$  and the utilized model is

$$\dot{x} = V \cos \psi \cos \theta, \quad (7)$$

$$\dot{y} = V \sin \psi \cos \theta, \quad (8)$$

$$\dot{z} = V \sin \theta, \quad (9)$$

$$\dot{V} = \frac{1}{m}(T - D - W \sin \theta), \quad (10)$$

$$\dot{\psi} = \frac{L \sin \varphi}{mV}, \quad (11)$$

where  $m$  is the weight,  $T = \|\mathbf{T}\|$ ,  $W = \|\mathbf{W}\| = mg$ .

A steady descending flight is assumed to be the best choice for the considered glide emergency landing [14]. Let assume the trajectory be divided into a set of segments with the fixed radii in which both the pitch and roll angles are constant. Moreover, the vertical acceleration is assumed to be zero, i.e.,  $\ddot{z} = 0$ , which enforces the lift force to counterweight the gravitational force, and thus

$$\frac{W \sin \varphi}{mV \cos \varphi \cos \theta} = \frac{V \cos \theta}{R}. \quad (12)$$

The pitch angle is assumed to be small, since it is maximized for the best gliding ratio ( $\theta < 0$ ). Therefore  $\cos \theta \approx 1$  and knowing  $W = mg$ , the roll angle can be approximated by

$$\varphi \approx \tan^{-1} \left( \frac{V^2}{Rg} \right). \quad (13)$$

The lift coefficient necessary for a steady flight is determined from (5) and (13) which gives

$$C_L = \frac{2W \sqrt{\left(\frac{V^2}{Rg}\right)^2 + 1}}{\rho S V^2 \cos \theta} = \frac{H}{\cos \theta}, \quad (14)$$

where  $H$  is considered to be constant for a fixed  $R$  and  $V$ . Then, the drag coefficient depends on the pitch angle and

$$C_D = C_{D0} + k \frac{H^2}{\cos^2 \theta}. \quad (15)$$

The speed of the aircraft is considered to be constant ( $\dot{V} = 0$ ) and there is not thrust ( $T = 0$ ), and thus using (10), the drag is compensated by the altitude loss ( $D + W \sin \theta = 0$ ) that can be expressed using (5) and (15) as

$$\left( C_{D0} + k \frac{H^2}{\cos^2 \theta} \right) = -\frac{2W \sin \theta}{\rho S V^2}. \quad (16)$$

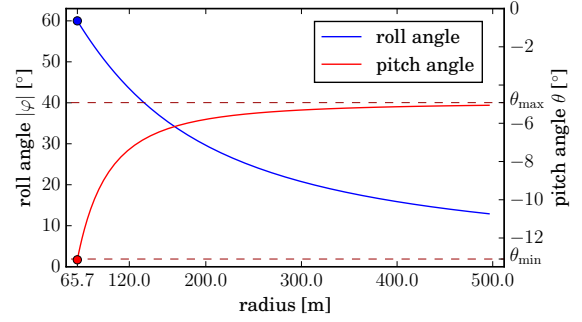


Fig. 4. Pitch and roll angles for turning maneuvers for Cessna 172 according to the selected turning radius  $R$ . The values were computed from (13) and (17) using the aircraft's parameters from Table I.

Finally, if the angle  $\theta$  is small, the approximation of  $\cos \theta \approx 1$  can be made and a closed-form expression can be found

$$\theta \approx -\sin^{-1} \left( \frac{\rho S V^2 (C_{D0} + k H^2)}{2W} \right). \quad (17)$$

However, for accurate results, (16) needs to be solved by a continuous optimization method, which is straightforward in this case, because it contains only a single variable  $\theta$ .

#### A. Altitude loss for Cessna 172

In this paper, we focus on the fixed-wing aircraft, and thus the selected one is the most popular aircraft Cessna 172 to verify a real behavior of the proposed approach. The aircraft basic parameters are summarized in Table I. The roll and pitch angles are computed for paths with various curvature given by the radius  $R$  from (13) and (17), see Fig. 4. The minimum turning radius is  $R_{\min} \approx 65.7$  m for  $\varphi_{\max} = 60^\circ$ . The pitch angle is the lowest (the steepest descent) for  $R_{\min}$  and the value is  $\theta_{\min} \approx -13.1^\circ$ . In contrast, the highest pitch angle (the shallowest descent) occurs for the straight path with  $\theta_{\max} \approx -4.9^\circ$ .

TABLE I  
TECHNICAL PARAMETERS OF CESSNA 172.

Parameter	Symbol	Value
Vehicle mass	$m$	1000 kg
Wing area	$S$	16.2 m <sup>2</sup>
Wing span	$b$	11 m
Span efficiency factor	$\epsilon$	0.8
Coefficient of geometric drag	$C_{D0}$	0.0341
Optimal glide airspeed	$v$	33.4 m·s <sup>-1</sup>
Lift-induced drag coef.	$k$	0.053
Maximum roll angle	$ \varphi_{\max} $	60°
Minimum turning radius	$R_{\min}$	65.7 m

#### B. Turning Radius Optimization for 3D Trajectory

First, the trajectory is determined by 2D Dubins maneuver [4] with a constant speed  $V$ . Then, the found 2D path is extended to the 3D trajectory such that the minimum possible altitude loss is computed and applied to the final trajectory. The altitude loss  $\mathcal{H}$  is defined based on the pitch angle  $\theta$  which depends on the horizontal curvature of the 2D path.

The Dubins maneuver is the shortest path in 2D, but it does not always provide the optimal solution according to the altitude loss. Therefore, the radii of the Dubins maneuver are

optimized for each generated maneuver separately. It leads to the following optimization problem where only CSC type of the Dubins maneuver [4] is allowed. Then, the altitude loss of the 2D Dubins maneuver is given by the sum

$$\mathcal{H}(R_1, R_3) = \sum_{i=1}^3 -\mathcal{L}_i \tan(\theta(R_i)), \quad (18)$$

where  $\mathcal{L}_1, \mathcal{L}_2, \mathcal{L}_3$  are 2D lengths of the maneuver segments and  $R_1, R_2, R_3$  are the radii of the segments. The second radius is  $R_2 = \infty$ , because it is the straight segment in CSC, i.e., the S segment. The optimization problem of finding the lowest altitude loss for various radii is defined as

$$\min_{R_1, R_3} \mathcal{H}(R_1, R_3). \quad (19)$$

#### IV. PROPOSED INFORMED RRT\*-BASED METHOD

The optimization criteria (2) of the proposed Problem 2.1 is to maximize the height of the aircraft above the terrain or obstacles during the flight. However, the aircraft glides and loses its altitude as it flies. Thus, the planning process needs to be very fast because the altitude lost during the computation may cause the aircraft would not be able to reach any landing site safely. We propose to employ a modified variant of the RRT\* algorithm [15] to address the following challenges raised from the formulated problem.

- 1) The start of the trajectory is given by the actual aircraft configuration that changes during the planning process.
- 2) Multiple landing sites are considered simultaneously.

We aim to provide an any-time planner, and thus the roadmap expansion from a root located at the current aircraft position cannot be used because every time the aircraft moves, the origin of the roadmap would change as well. Therefore, we propose to grow the roadmap from the landing site towards the aircraft. Thus, we consider a dual problem formulation to Problem 2.1 where the lowest safety altitude  $\mathcal{A}(q_{\text{act}})$  for a successful landing has to be found for the current aircraft position  $q_{\text{act}}$ , see Fig. 2. This provides the desired any-time property for planning the emergency landing trajectory during the flight, even before the loss of thrust.

The second challenge is addressed by creating multiple trees with roots at the landing sites. Thus, a forest of the planning trees is created, but it can also be seen as one compact tree if all the landing sites are connected to a single virtual root. The values associated to edges that connect the roots with the virtual root correspond to the altitude of the specific landing site as the lowest altitude  $\mathcal{A}$  has to be minimized.

Besides, we propose to simplify the complexity of the planning problem by a reduction of the configuration space dimensionality that is based on the aircraft model described in Section III. Thus, the pitch angle  $\theta$  and roll angle  $\varphi$  are not considered because they can be adjusted easily compare to the heading angle  $\psi$ . Further, the altitude  $z$  is not contained in the reduced configuration space for the roadmap construction since it is optimized as the minimum safety altitude  $\mathcal{A}$  in the cost function. Therefore, the proposed

---

#### Algorithm 1: RRT\* for Emergency Landing

---

**Input:**  $\Xi = \{\xi_1, \dots, \xi_n\}$  – the set of landing sites  
**Input:**  $\tilde{q}_{\text{act}}$  – the current position of the aircraft  
**Output:**  $\Gamma$  – the best emergency landing trajectory

```

1  $G \leftarrow \{V \leftarrow \Xi \cup v_{\text{virt}}, E \leftarrow \bigcup_i^n (v_{\text{virt}}, \xi_i)\}$ 
2  $\mathcal{A}(\xi_i) \leftarrow \mathcal{T}_{\text{alt}}(\xi_i), \forall \xi_i \in \Xi$ 
3 while IsMotorRunning() do
4    $\tilde{q}_{\text{act}} \leftarrow \text{UpdateAircraftConfiguration}()$ 
5    $\tilde{q}_{\text{rand}} \leftarrow \text{SampleInformed}(\Xi, \tilde{q}_{\text{act}})$ 
6    $\tilde{q}_{\text{nearest}} \leftarrow \text{Nearest}(\tilde{q}_{\text{rand}}, G)$ 
7    $\tilde{q}_{\text{new}} \leftarrow \text{Steer}(\tilde{q}_{\text{nearest}}, \tilde{q}_{\text{rand}})$ 
8    $Q_n \leftarrow \text{Near}(\tilde{q}_{\text{new}}, G)$ 
9    $\tilde{q}_* \leftarrow \text{argmin}_{\tilde{q}_n \in Q_n} [\mathcal{A}(\tilde{q}_n) + \mathcal{H}(\tilde{q}_{\text{new}}, \tilde{q}_n)]$ 
10   $\mathcal{A}(\tilde{q}_{\text{new}}) \leftarrow \max[\mathcal{T}_{\text{alt}}(\tilde{q}_*, \tilde{q}_{\text{new}}), \mathcal{A}(\tilde{q}_*) + \mathcal{H}(\tilde{q}_{\text{new}}, \tilde{q}_*)]$ 
11   $V \leftarrow V \cup \{\tilde{q}_{\text{new}}\}; E \leftarrow E \cup \{(\tilde{q}_*, \tilde{q}_{\text{new}})\}$ 
12   $G \leftarrow \text{Rewire}(Q_n, G)$ 
13   $G \leftarrow \text{RemoveUnreachableSamples}(G)$ 
14  $Q_n \leftarrow \text{Near}(\tilde{q}_{\text{act}}, G)$ 
15  $\tilde{q}_{\text{best}} \leftarrow \text{argmin}_{\tilde{q}_n \in Q_n} [\mathcal{A}(\tilde{q}_n) + \mathcal{H}(\tilde{q}_{\text{act}}, \tilde{q}_n)]$ 
16  $\Gamma \leftarrow \text{RetrieveFinalTrajectory}(\tilde{q}_{\text{act}}, \tilde{q}_{\text{best}}, G)$ 

```

---

simplified configuration  $\tilde{q}$  consists of only 2D position  $(x, y)$  and the heading angle  $\psi$ ,  $\tilde{q} = (x, y, \psi)$ ,  $\tilde{q} \in SE(2)$ , which significantly reduces the computation burden of the RRT\*.

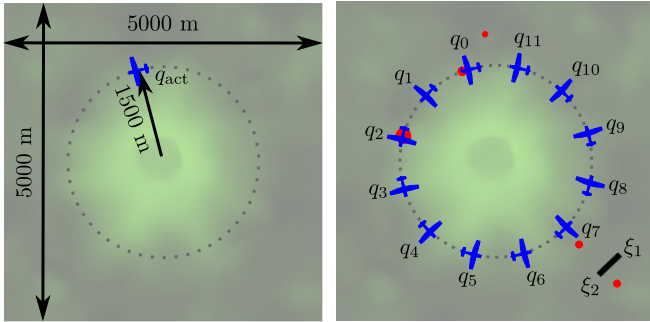
The overall structure of the proposed RRT\*-based algorithm for the emergency landing is listed in Algorithm 1. The algorithm is initialized by inserting all possible landing sites into the graph  $G$ . The minimum altitude  $\mathcal{A}$  to land on the site  $\xi_i$  is set to its altitude  $\xi_i^{\text{alt}}$ . After the initialization, the main cycle of the roadmap expansion starts and runs until any problem of the plane is detected, which is indicated (IsMotorRunning()). The structure of the algorithm is similar to the original RRT\*, but the collision checking procedure is removed because the aircraft can fly over the obstacles if its altitude is sufficiently high. Besides, a possible collision means an undesirable altitude of the aircraft which can be easily checked for  $\mathcal{T}_{\text{alt}}(\Gamma_{2D}(t))$  in (1). Therefore, the minimum altitude  $\mathcal{L}_{\text{alt}}(\tilde{q}_i, \tilde{q}_j)$  for a flight from  $\tilde{q}_i$  to  $\tilde{q}_j$  is utilized. Such an altitude guarantees a safe landing and also maximizes the height of the aircraft.

In the first step of the roadmap expansion, a random sample is selected in the SampleInformed() procedure based on the informed strategy adopted from [12]. An elliptical region is used to exclude samples which cannot contribute to the best solution. This concept is further extended to consider the multiple landing sites simultaneously as follows. Let  $\mathcal{A}(\tilde{q}_{\text{act}})$  be the current best solution for the current configuration  $\tilde{q}_{\text{act}}$  to the selected landing site. Then, the samples are selected for each landing site  $\xi_i$  separately, but each generated sample  $\tilde{q}_{\text{rand}}$  is checked to fulfill the equation

$$\mathcal{A}(\tilde{q}_{\text{act}}) \geq d[\mathcal{E}(\tilde{q}_{\text{act}}, \tilde{q}_{\text{rand}}) + \mathcal{E}(\tilde{q}_{\text{rand}}, \xi_i)] + \mathcal{T}_{\text{alt}}(\xi_i) - \delta_{\mathcal{A}}, \quad (20)$$

where  $\mathcal{E}$  is the Euclidean distance between 2D projections of the samples,  $\mathcal{T}_{\text{alt}}(\xi_i)$  is the altitude of the specific landing site  $\xi_i$ ,  $d = -\tan(\theta_{\text{max}})$  is the minimum glide ratio given





(a) Dimensions in the scenario and the flight plan trajectory. (b) Selected aircraft's configurations and possible landing sites.

Fig. 5. An experimental scenario utilized for testing.

by  $\theta_{max}$ , and  $\delta_{\mathcal{A}}$  represents a slight extension of the region because the aircraft is moving during the planning process.

After a random sample  $\tilde{q}_{rand}$  is determined, the nearest configuration  $\tilde{q}_{nearest}$  is selected in the `Nearest()` procedure using the length of the 2D Dubins maneuver. Subsequently, the tree is expanded from  $\tilde{q}_{nearest}$  towards  $\tilde{q}_{rand}$  by the `Steer()` procedure in which a 2D Dubins maneuver is generated. If the maneuver is longer than the given steer coefficient, the maneuver is shortened, and a new sample  $\tilde{q}_{new}$  is generated at the maneuver ends. The best predecessor to  $\tilde{q}_{new}$  is selected from the candidate samples by the procedure `Near()`. Then, the best predecessor sample is chosen to minimize the required altitude  $\mathcal{A}$  which is influenced mainly by the terrain altitude and the altitude loss  $\mathcal{H}$  from the predecessor sample.

The solution is improving by updating the tree if the newly inserted node can improve the value of  $\mathcal{A}$  for any subsequent samples. Such optimization is done in the `Rewire()` procedure in which all the samples from the neighborhood  $Q_n$  of the inserted sample  $\tilde{q}_*$  are examined to be reconnected to  $\tilde{q}_*$  and minimize  $\mathcal{A}$ . However, all new connections need to be tested against the terrain and obstacles given by  $\mathcal{T}_{alt}$ .

Notice that the memory requirements of the algorithm are reduced by pruning the roadmap. Thus, if any sample or a sub-tree are not reachable anymore by the aircraft it is removed from the graph  $G$  in the `RemoveUnreachableSamples()` procedure, which supports the algorithm running during the whole flight.

In the case, the aircraft experiences the LoT, the expansion of the roadmap is terminated, and the final trajectory is determined. This process is analogous to inserting a new sample to the roadmap; but in this case, a complete trajectory is retrieved from  $G$  in `RetrieveFinalTrajectory()` procedure. Nevertheless, only a limited neighborhood around the actual position of the aircraft is checked, and thus the final emergency landing trajectory is retrieved almost instantly (about 80 ms), whenever the emergency landing is requested.

## V. RESULTS

A terrain scenario with obstacles has been prepared to verify and evaluate the performance of the proposed any-time planning approach for safe emergency landing planning using the RRT\*. The scenario consists of a conical volcano with the height of 1000 m that is surrounded by relatively

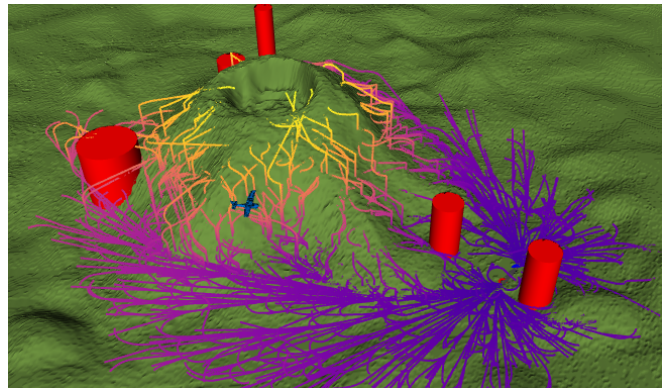


Fig. 6. An example of the problem instance with the RRT\* tree representing possible emergency landing trajectories retrieved by the proposed any-time algorithm during the third round around the volcano. The growth of the tree and more information can be seen in the attached video.

flat terrain with altitudes in the range from 0 to 250 meters. Besides, there are five cylindrical obstacles with the height from 450 to 750 meters and radius in between 100 and 250 meters placed within 2.7 km from the center of the volcano. A single bi-directional runway with the oppositely oriented landing sites  $\xi_1$  and  $\xi_2$  is located close to the base of the volcano. The scenario is visualized in Fig. 5.

The used maneuvers in the roadmap are based on the Dubins maneuvers of the CSC type that were optimized regarding the turning radius and altitude loss as described in Section III and Section IV. A discrete set of 10 various radii within the interval  $R_i \in [R_{min}, 6R_{min}]$  are considered, and the trajectory with the lowest altitude loss  $\mathcal{H}$  is selected from 100 combinations.

In the evaluation scenario, the aircraft is flying at the altitude of 800 m around the volcano along the circular trajectory with the radius of 1500 m, and thus a gliding trajectory over the volcano is impossible. Besides, 12 configurations  $\{q_0, \dots, q_{11}\}$  along the circular flight path where the engine malfunction may occur have been selected such that the spacing between them corresponds to 23.5 seconds of the flight. The first configuration  $q_0$  is visited at the time 0 s, and then, the aircraft continues to  $q_1$ , etc. An example of the utilized scenario is depicted in Fig. 6.

The proposed algorithm has been evaluated together with its single-query variant with a limited computational time that plans the landing trajectory from the current aircraft position. The proposed any-time algorithm returns the landing trajectory almost instantly in about 80 ms because the roadmap of the RRT\*-based algorithm is already populated. On the other hand, the single-query variant starts with an empty roadmap, and it needs to build the whole roadmap; however, the aircraft is already losing the altitude until the final trajectory is produced. This altitude loss influences the overall performance of the single-query variant and disadvantages it against the proposed any-time variant, especially for longer computational times.

The circle flight plan has been repeated three times for the proposed algorithm which gives a sufficient time to build the roadmap of reasonable quality. All the results have been

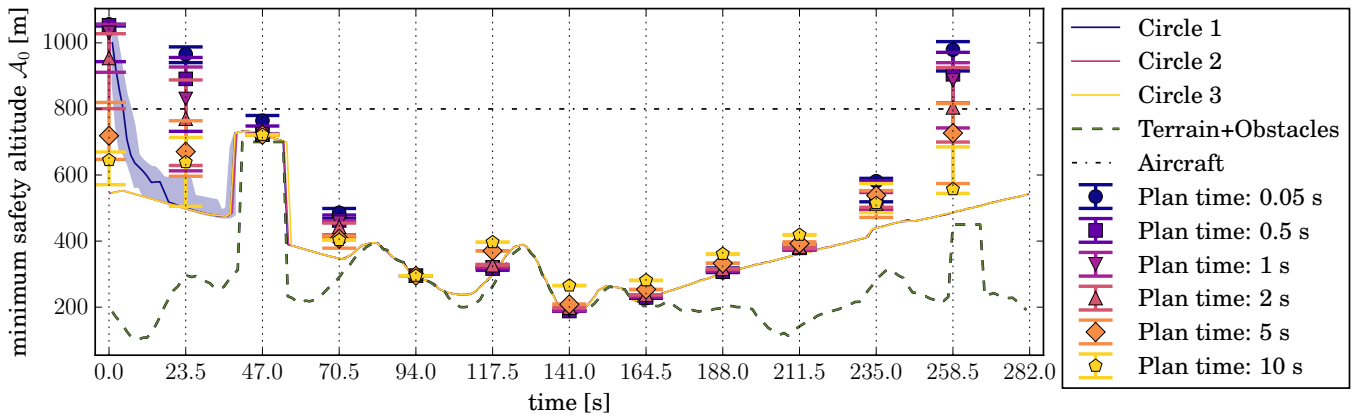


Fig. 7. The minimum safe altitude of the found trajectories obtained by the proposed any-time algorithm and its single-query version for different planning times. Median and 90% non-parametric confidence interval from 40 trials are shown together with the altitude of the terrain/obstacles and the flight level of the aircraft. If the minimum safe altitude of the trajectory is above the hatched line of the aircraft level, the trajectory is unfeasible.

evaluated 40 times on a single core of AMD Phenom II X6 1090T CPU running at 3.2 GHz, and the overview of the results can be seen in Fig. 7.

#### A. Discussion

Although the aircraft can safely land from any position along its trajectory, the single-query version of the solver is unable to find a feasible solution if the dedicated time to find a solution is too short. In such cases, the minimum required altitude is higher than the current altitude of the aircraft.

In the first round, the proposed algorithm starts with similar results as the single-query version because no roadmap is pre-computed yet. Starting from the third configuration  $q_2$ , the proposed algorithm returns almost the same results for all the rounds because the roadmap is already dense enough and a high-quality solution can be provided almost instantly.

In contrast, the single-query version struggles in configurations  $q_0$ ,  $q_1$ , and  $q_{11}$  which are far from the airport and it needs to be determined from which side the volcano is flown around. Interestingly, the single-query version returns a solution with higher quality for these three configurations if more computational time is provided, but it is not always the case. Contrarily, for the configurations  $q_6$  to  $q_9$ , a higher required computational time causes that worse solutions are found because the aircraft is heading from the airport and it needs to be turned around as soon as possible.

The results support the proposed any-time algorithm vital, and it combines advantages of both the single-query planning to find a high-quality solution but with the faster response than the pure single-query planning. Therefore, there is no need to defined the maximal computational time since the roadmap is expanding continuously during the flight.

#### VI. CONCLUSION

A novel any-time RRT\*-based approach for planning a safe emergency landing trajectories is proposed in this paper. The proposed solution outperforms the single-query approach because the roadmap with all possible landing trajectories is continuously updated during the flight and if the LoT occurs, the found landing trajectory can be returned instantly. This gives the human pilot time to solve other

issues than selecting the most suitable landing site. As a byproduct, the proposed approach returns the minimum safe altitude from which the plane can glide to at least one of the available landing sites. It may be used to inform the pilot to climb to a safe altitude to have a safe emergency landing trajectory should the LoT occurs.

#### REFERENCES

- [1] J. D. Kenny, *26th Joseph T. Nall Report*. Richard G. McSpadden, JR., 2017.
- [2] *Loss of Thrust in Both Engines After Encountering a Flock of Birds and Subsequent Ditching on the Hudson River*. National Transportation Safety Board, 2009.
- [3] S. Paul, F. Hole, A. Zytek, and C. A. Varela, "Flight Trajectory Planning for Fixed-Wing Aircraft in Loss of Thrust Emergencies," *arXiv preprint arXiv:1711.00716*, 2017.
- [4] L. E. Dubins, "On curves of minimal length with a constraint on average curvature, and with prescribed initial and terminal positions and tangents," *American Journal of mathematics*, vol. 79, no. 3, pp. 497–516, 1957.
- [5] H. Chitsaz and S. M. LaValle, "Time-optimal paths for a dubins airplane," in *IEEE CDC*, 2007, pp. 2379–2384.
- [6] N. Meuleau, C. Plaunt, D. Smith, and T. Smith, "Emergency landing planning for damaged aircraft," in *Innovative Applications of Artificial Intelligence Conference*, 2009, pp. 3247–3259.
- [7] P. Eng, "Path planning, guidance and control for a uav forced landing," Ph.D. dissertation, Queensland University of Technology, 2011.
- [8] S. Choudhury, S. Scherer, and S. Singh, "RRT\*-AR: Sampling-based alternate routes planning with applications to autonomous emergency landing of a helicopter," in *ICRA*. IEEE, 2013, pp. 3947–3952.
- [9] P. F. Di Donato and E. M. Atkins, "An off-runway emergency landing aid for a small aircraft experiencing loss of thrust," in *AIAA Infotech@ Aerospace*, 2015, p. 1798.
- [10] E. M. Atkins, D. Berenson, I. V. Kolmanovsky, D. Panagou *et al.*, "Toward autonomous aircraft emergency landing planning," Ph.D. dissertation, University of Michigan, 2017.
- [11] M. Coombes, W.-H. Chen, and P. Render, "Reachability analysis of landing sites for forced landing of a uas," *Journal of Intelligent & Robotic Systems*, vol. 73, no. 1-4, pp. 635–653, 2014.
- [12] J. D. Gammell, S. S. Srinivasa, and T. D. Barfoot, "Informed RRT\*: Optimal sampling-based path planning focused via direct sampling of an admissible ellipsoidal heuristic," in *IROIS*, 2014, pp. 2997–3004.
- [13] R. W. Beard and T. W. McLain, *Small unmanned aircraft: Theory and practice*. Princeton University press, 2012.
- [14] N. H. McClamroch, *Steady aircraft flight and performance*. Princeton University Press, 2011.
- [15] S. Karaman and E. Frazzoli, "Sampling-based algorithms for optimal motion planning," *The International Journal of Robotics Research*, vol. 30, no. 7, pp. 846–894, 2011.